WIND-TURBINE LUBRICATION

Low temperature fretting wear behavior of four commercial greases

By JIE ZHANG, ALAN WHEATLEY, RIHARD PASARIBU, EDWARD WORTHINGTON, SARAH MATTHEWS, CAROLINE ZINSER, and PHILIPPA CANN

Wind turbines play an increasingly important role in the global energy market. The World Wind Energy Association [1] reported yearly growth of 13 percent in 2021 to an overall capacity of 840 GW, enough to provide more than 7 percent of the global power requirement. Operating requirements are becoming more demanding with the move toward larger structures, higher loads, increased off-shore development and hostile environmental conditions. Downtime is expensive both in lost energy production and repair costs, particularly for off-shore turbines. Wind turbines are particularly prone to gearbox failure and a recent paper [2] reported more than 50 percent of this is due to bearing problems. Rolling bearings in wind turbines are in the gearbox, shaft, pitch/blade, yaw, and generator systems, where they are often subject to extreme operating conditions of high loads, low temperatures, and variable wind speeds [2]. Various lubrication-related failure modes have been identified, including scuffing, micro-pitting, and fretting corrosion [2], [3].

1 WIND TURBINE TRIBOLOGY

Both grease and oil lubricants are used in wind-turbine systems; grease is the main lubricant in the pitch/yaw, generator, and shaft bearings, and formulated oil is in the gearbox. One of the challenges is to optimize grease formulation for such demanding conditions, particularly low-temperature operation.

The focus of this article is the low-temperature lubrication of the pitch and yaw bearings, as they can fail due to fretting/corrosion and false brinelling [2] damage. Fretting is defined as "small amplitude relative oscillatory motion between two contacting bodies that gives rise to both wear and fatigue" [3]. It is associated both with low amplitude motion and system vibration. The origins of oscillation and fretting in bearings are due to the operating requirements of the turbine.

While most bearings rotate, oscillation is not uncommon. In some applications, the oscillation is intended and fairly large. The pitching system for wind-turbine blades is an example. The blade angle is changed to accommodate changes in wind speed and keep the rotating speed of the propeller within acceptable limits. In older, smaller wind turbines, the angle was changed based on the overall wind speed, and the changes were not very frequent. In the more modern, larger wind turbines, the blade angle is often changed during the rotation. This helps to compensate for differences in wind speed at different heights during the rotation and is known as active pitching [3]. There are many examples of unintended oscillation. In wind-turbine blade bearings, for example, at the top of the rotation, the blade is pushing down, axially on the bearing. At the bottom of the rotation, it is pulling the bearing axially in the opposite direction, which leads to a small axial movement. Other oscillations can be caused by wind-speed changes (gusting) and offshore wave motion.

The bearings in the blade pitch system are usually four- or eight-point contact rolling bearings [2]. Stammler et al. [3] [4] provided an analysis of pitch angle rotation for a 7.5-MW turbine blade bearing; this was a 4,690 mm diameter double row bearing with 80 mm diameter balls. The pitch oscillations are low frequency and typical pitch angle of a few degrees (<2°). The analysis concluded that 15.3 percent of all pitch movements occur between angles of 0.03° and 0.2° [4], which correspond to fretting conditions.

Fretting occurs when the reciprocating motion (L) is less than the Hertzian contact width (2a) [3], [4], [5] (Figure 1), which has implications both for the formation and behaviour of wear particles [5] and the ability of the lubricant to generate a separating film. The restricted motion means wear particles generated during rubbing are not expelled from the contact zone and remain actively involved in the lubrication process [5]. A second outcome is reduced entrainment of lubricant impeding the development of a sufficient

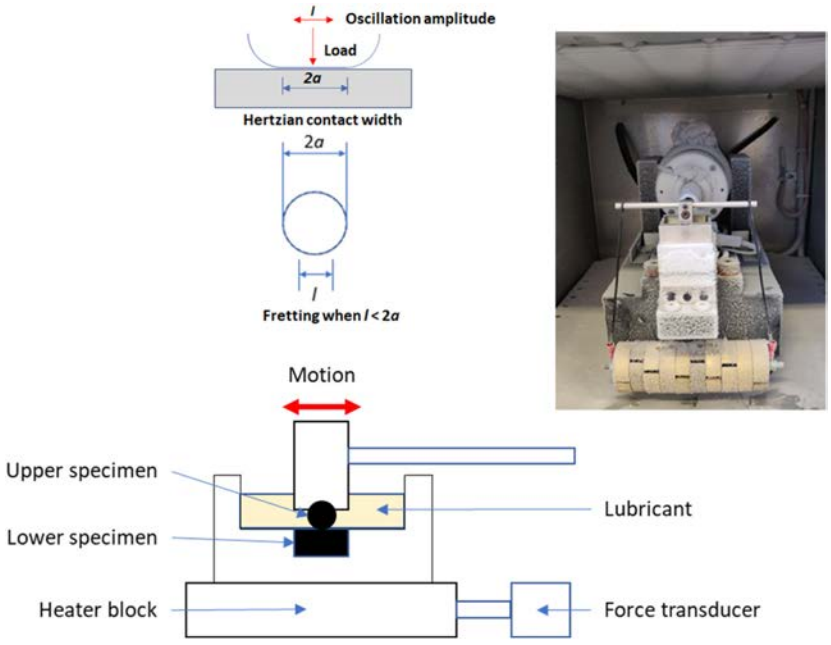

Figure 1: HFRR test device: fretting condition, simple schematic and installed in the freezer.

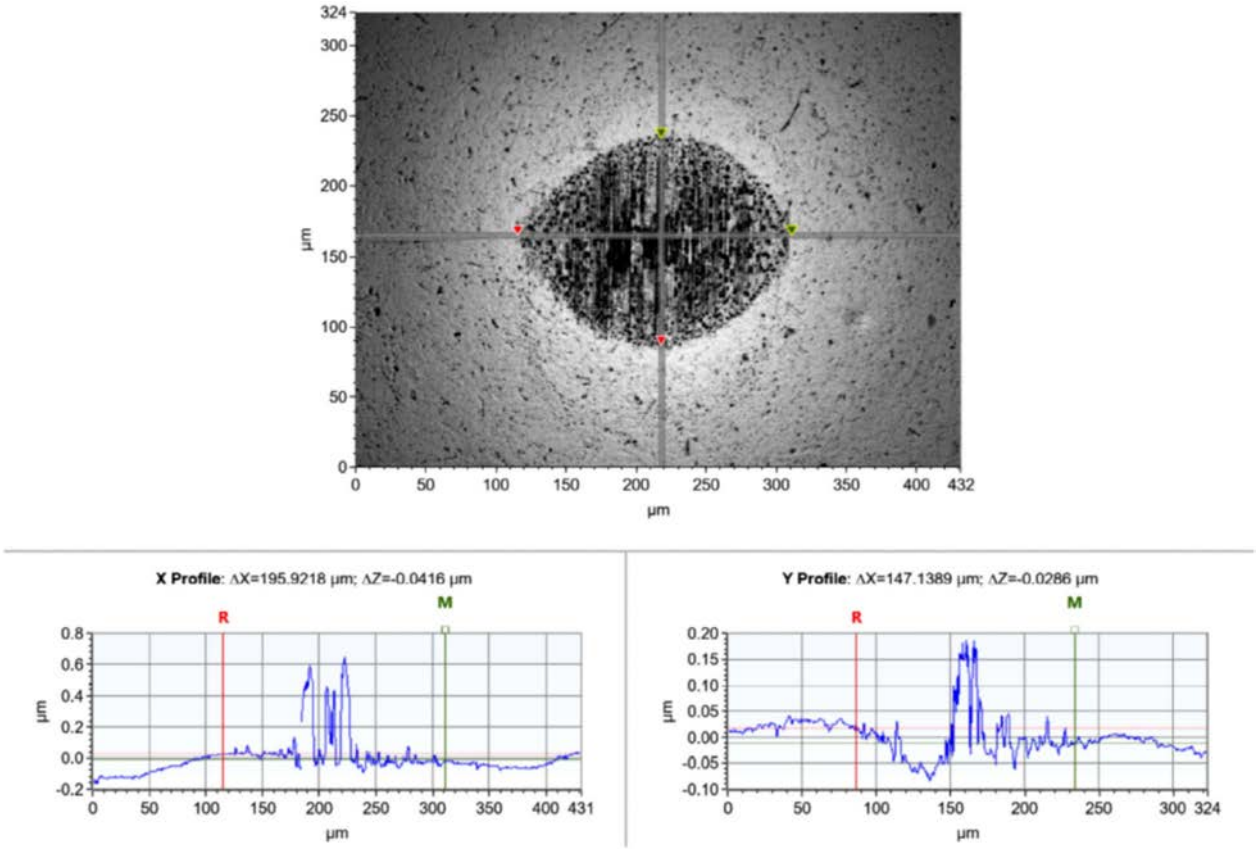

Figure 2: Wear measurement using SWLI.

lubricating film as the restricted motion and low speed combine to hinder the formation of an elastohydrodynamic lubricating (EHL) film [6].

Greases used in wind turbine bearings typically use calcium or lithium-based thickeners with either mineral oil or synthetic hydrocarbon base oils. Several standard tests are used to assess grease fretting performance. ASTM D4170 [7], known as the Fafnir fretting test, measures wear in thrust bearings run at a frequency of 30 Hz, 12°arc of motion and room temperature. Bearing wear is measured by weight loss. A second test ASTM D7594 [8] uses a reciprocating ball-on-flat bench test (SRV) to measure friction and wear typically at 50 °C, 0.3 mm stroke, 50 Hz and 2.2 GPa. Neither of these tests is usually run at low temperatures representative of wind turbine operation. The NLGI have published a specification guide (HPM+LT) for greases used at low temperatures [9]. The tests include ASTM D1478 which is a low temperature (30 °C) ball bearing torque test and other flow/grease mobility tests [9]. A low temperature fretting test appropriate for wind turbine applications is not specified. At present none of the industry tests accurately reproduces the fretting conditions in low-temperature wind turbines.

A number of papers have reported grease lubrication under fretting conditions both in bearings and ball-on-disc tests [10], [11], [12]. The Schwack et al. study [10] focused on conditions in wind turbine pitch blade bearings and compared measurements in a bearing and SRV bench test for six commercial greases. The greases had a range of thickener types (calcium/calcium complex, lithium/lithium complex) and base oil viscosities/composition. The bearing tests were run at fretting (L/2a=0.9) and sliding conditions (L2a=13.3, 29.2). The SRV tests were run at L/2a = 1 at 8 and 32 Hz, stroke length 0.3 mm and 20 °C. The overall conclusion was that greases with low base oil viscosity and high bleed rates gave the best fretting wear performance which is in line with other studies [11][12].

Despite the importance of wind turbine technology and the increasing power demands, currently we do not have a simple bench-test which will replicate wind turbine bearing fretting at different temperatures. The aim of the current work was to address this problem through the development of a bench-top fretting test which could be run at very low temperatures, down to minus-40°C. The tests were designed to replicate low amplitude fretting in bearings under realistic operating conditions.

A series of ball-on-disc reciprocating fretting tests was carried out to investigate the friction and wear properties of four greases at different temperatures (25, 7, minus-20, mi-

nus-40°C). Post-test the wear scar and grease distribution on the disc was examined by a low-power microscope. The wear scar dimensions on the ball were determined by White Light Interferometer (WLI). Further analysis was carried out to understand grease lubrication mechanisms under fretting conditions. The chemical composition of the grease film in the wear scar was analysed by Reflection Absorption Fourier Transform Infrared Spectroscopy (RA-IRS). The disc was then cleaned, and Raman Spectroscopy and SEM-EDS used to examine the surface chemistry of the wear scar.

HFRR test conditions.

Test condition	Value
Temperature (°C)	25, 7, – 20 and – 40
Load (g)	1000
Number of strokes	100k
Frequency (Hz)	25
Stroke length (µm)	100
Average speed	5 mm/s (mid point 7.85 mm/s)
Contact Pressure (GPa)	1.4
Grease sample thickness	50 µm thick, 4 mm diameter

Table 1: HFRR test conditions.

2 TEST METHODS AND MATERIALS

2.1 Friction and wear tests

The High Frequency Reciprocating Rig (HFRR) [PCS Instruments, Acton, UK] was initially designed for evaluating diesel fuel lubricity as described in ASTM D6079 and ISO 12156 [13], [14]. It has also been extensively used to evaluate wear and friction properties of a wide range of lubricants, additives and greases. The HFRR set-up is schematically shown below in Figure 1, in which a steel ball (6 mm diameter) is loaded and reciprocated against a stationary steel disc (10 mm diameter).

The surface roughness (Ra) of the ball and disc specimens was 9.9±1.2 nm and 4.8±0.8 nm respectively; while the hardness of the ball and disc specimens was 800 Hv and 196 Hv respectively. The ball is driven by an electromagnetic vibrator to achieve oscillating motion at desired frequency and stroke length. A temperature probe is under the disc specimens to monitor the test temperature. A force transducer mounted underneath the heater block measures real-time friction force throughout the test. Before testing, metal specimens were cleaned in an ultrasonic bath with toluene, rinsed in acetone, and air-dried. At least three tests per condition were run.

The formation of a tribofilm or any change to the contact between the ball and disc specimens was indicated by the electrical contact resistance (ECR). The ball-disc contact resistance is related to ball-disc contact geometry, resistance of lubricant, and/or specimen materials, and formation of a tribofilm. During a HFRR test, a constant electrical potential of approximately 15 mV is applied to the ball and disc contact with a balance resistor connected in series. Therefore, when the ball and disc are fully separated (open circuit), the voltage will be c.a. 15 mV, representing 100 percent film; while, when there is direct metal-to-metal contact between the ball and disc, the voltage will be 0 V, representing zero percent film. Although ECR does not provide a direct measurement of film thickness in association with friction and wear results, it can provide insights into possible lubrication and wear mechanisms.

To replicate grease lubrication conditions occurring in wind turbine bearings it is necessary to control a number of parameters, these include stroke length for fretting, temperature, and initial grease sample application.

Liquid lubricant tribology tests are usually run with an excess of fluid present. However, in bearings, there is a very small amount of grease situated close to the contact and lubricant replenishment of the raceway is often limited [16], [17]. For most liquid lubricant tests, it is sufficient to replicate the speeds, temperature, contact pressure, etc. For greases, it is also necessary to consider the mechanisms driving lubricant replenishment of the rubbed track. Clearly, this is only really achieved in full-scale bearing tests; the aim of the HFRR test design was to replicate the relevant conditions (motion/temperature/pressure), and lubricant distribution around the contact. To replicate this condition in the HFRR test, the grease sample was applied as a thin film on the disc. If an excess of grease is used, it can be dragged back into the contact zone by the ball holder, rather than the ball motion. By using a controlled, thin film sample, the aim was to test the ability of the grease to be retained in the contact or replenish the rubbed track after it is displaced during fretting. To meet this requirement, the grease was applied as a circular spot (4 mm diameter and 50 µm thick) on the disc.

The HFRR test conditions are listed in Table 1.

2.2 Post-test analysis

2.2.1 Wear analysis

A Bruker Scanning White Light Interferometer (SWLI) Contour GT was used to quantify wear scar diameter (WSD) on the ball after the HFRR tests. It uses scanning white light interferometry to map surface topography to sub-nanometer resolution. An example of ball WSD measurement is shown in Figure 2. The SWLI scans the topography of ball surface sector, which includes the wear scar, and the analyzing software fits the curvature of the surface using the ball radius of 3 mm. The fitted surface is thus a plane as shown in the top picture in Figure 2. Green and red cursers are then located on the edge of the wear scar to measure the lengths between them. The WSD was the average horizontal and vertical lengths of the ball wear scar. In Figure 2 the horizontal and vertical lengths of the ball wear scar are 195.9 µm and 147.1 µm so that the average WSD is 171.5 µm.

2.2.2 Grease composition analysis: FTIR and RA-IRS spectroscopy

Fourier Transform Infrared Spectroscopy (FTIR) is used to characterize and identify chemical species particularly for

organic compounds. In this study, it was used to detect thickener and base oil components of the greases [16]. A PerkinElmer Frontier FTIR equipped with an IR microscope was used. Fresh greases were also analyzed and used as reference spectra for the thickener/base oil content. Post-test grease films remaining in the disc wear track were examined using the IR microscope. The sample is first observed using the visual function and the sample area defined by a 100 µm diameter aperture. The microscope is then switched to the IR mode and the sample area scanned using the reflection-absorption method RA-IRS (Reflection-Absorption Infrared Spectroscopy). The in-track spectra were compared to the fresh grease reference to identify any changes in composition due to rubbing.

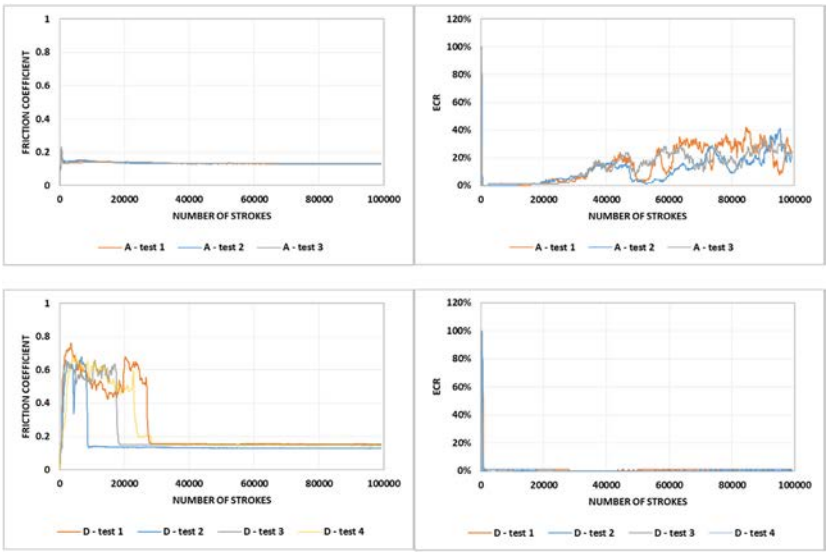

Figure 3: Example friction coefficient and ECR traces for greases A (upper) and D (lower) at 25°C.

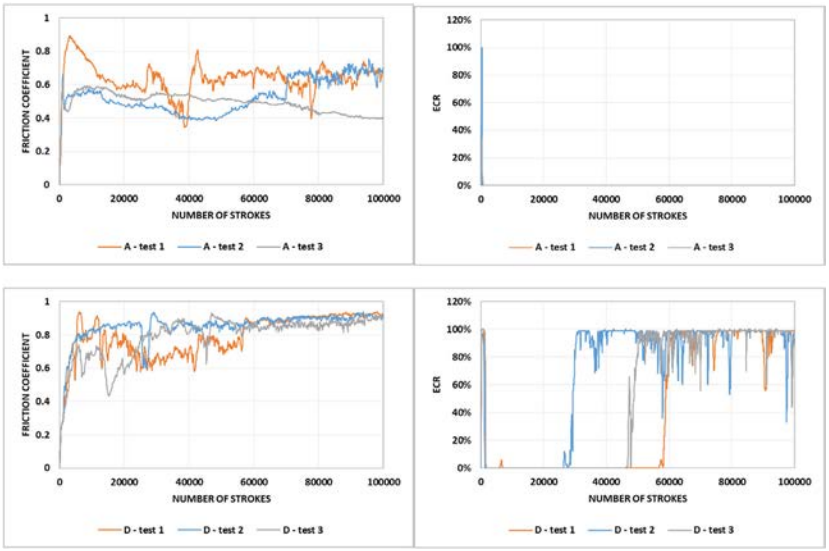

Figure 4: Example friction coefficient and ECR traces for greases A (upper) and D (lower) at minus-40°C.

2.2.3 Analysis of wear scar surface chemistry: Raman spectroscopy and SEM-EDS

Raman Spectroscopy was used to identify chemical species in both organic and inorganic compounds. An Alpha 300 RA (WiTec, Germany) with a 532 nm laser source was used to analyze the disc wear tracks after the HFRR tests, to investigate the formation of iron oxide films [18]. The samples were solvent-cleaned and spectra taken from different points in the wear scar. Representative results are shown in the paper for this analysis.

Raman spectroscopy was used to identify iron oxides in the wear track; however, additive tribofilms formed in the disc wear tracks were not identified. Scanning Electron Microscopy with Energy Dispersive X-ray Spectroscopy (SEM-EDS) was therefore used to investigate the element composition of the disc wear tracks. SEM enables a high-resolution image of the wear track, thus the same area of the wear track, which were studied with Raman, could also be analysed by EDS to determine the chemical composition. A Tescan Mira SEM-EDS (Kohoutovic, Czech Republic) was used to take high magnification and resolution images and detect elemental composition in the HFRR disc wear tracks.

2.3 Materials

Four greases were investigated, details of which are in Table 2. The greases chosen were commercially available from

Grease test samples: thickener types and base oil viscosity.

Greases	Thickener Type	Base oil η (mm²/s) 25 °C	7 °C	-20 °C	-40 °C
A	Calcium	23.3	57.6	433	4486
B	Lithium/calcium borate complex	224	706	7832	104,707
C	Lithium	316	1227	22,712	575,665
D	Lithium diacid complex	1116	4129	59,513	964,465

Table 2: Grease test samples: thickener types and base oil viscosity.

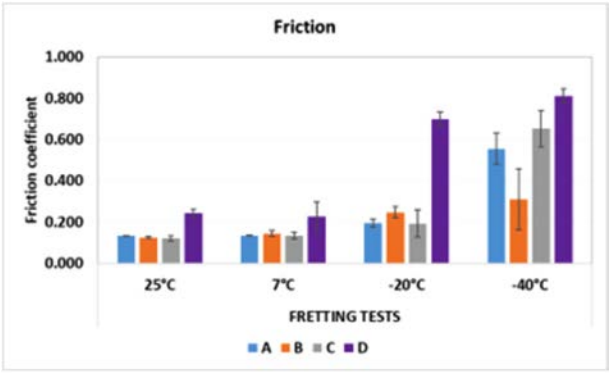

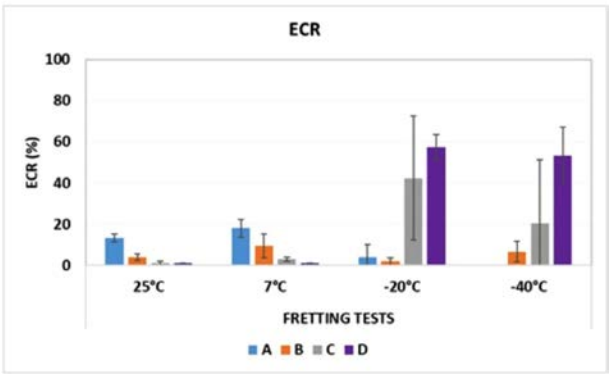

Figure 5: Averaged friction (upper) and ECR (lower) results.

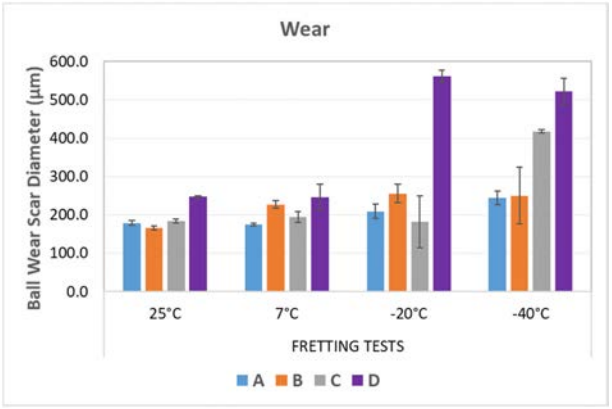

Figure 6: Summary of ball wear scar diameter measurements.

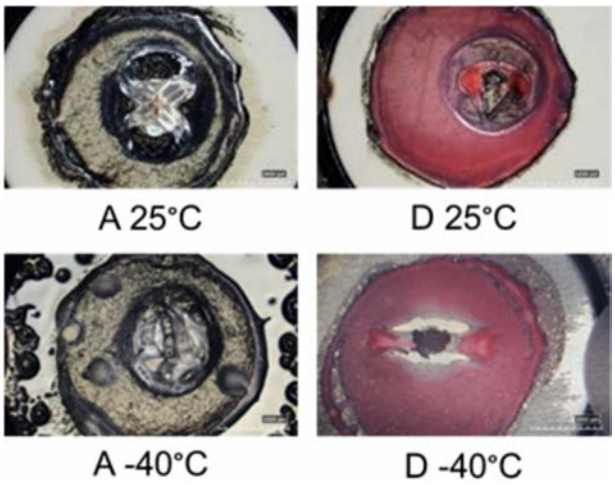

Figure 7: Images of the disc wear scar and grease films for A and D tests at 25°C (upper) and minus-40°C (lower). Scale marker: 2,000 µm.

different manufacturers and representative of formulations currently used in wind turbines. All the greases were hydroxstearate-based with calcium (A, B) or lithium/lithium complex (B, C, D) thickener chemistries. As these were commercial samples, it was not possible to obtain the base oils for viscosity measurements, so the base oil viscosities at minus-20 and minus-40°C quoted in Table 2 were calculated using the ASTM viscosity-temperature chart based on the published viscosities measured at other temperatures.

3 RESULTS AND DISCUSSION

3.1 HFRR friction and wear results

Friction and ECR values were recorded throughout the test and are typically plotted against time or number of strokes. At least three tests were carried out for each grease/temperature combination. Overall, the results were very repeatable; examples are shown in Figure 3, Figure 4 for greases A and D at 25 and minus-40°C, as these represent the performance extremes.

At the higher temperatures (25 and 7°C) the friction coefficient was low and stable for A, B, and C (<0.25). The exception was grease D, where the CoF was initially high (µ=0.5-0.8) and unstable; it then declined suddenly to a steady value (µ~0.15) for most of the test. Grease A ECR value increased steadily after 40,000 strokes (see Figure 3 upper graph) to values of 20-60 percent, which might indicate the development of a reacted additive film. For the lower temperatures (minus-20, minus-40°C), friction traces became increasingly high and unstable. Examples are shown in Figure 4 for A and D at minus-40°C. At minus-40°C, greases B, C, and D had very high, unstable friction and ECR traces. The exception was grease A, where the ECR trace was zero.

The test average friction coefficient and ECR results are plotted in Figure 5. The friction chart shows that, at higher temperatures (25 and 7°C), the four test greases presented comparable friction coefficient (µ ~0.15), with slightly higher values for grease D (µ > 0.2). At minus-20°C, greases A, B, and C gave mixed results, the CoF was often unstable and varied in the range µ=0.18–0.6. Grease D gave very high (µ=0.6–0.8), unstable friction traces in all tests. At minus-40°C, all greases gave very high average friction coefficients (0.5–0.8).

Figure 5 (lower graph) shows the average ECR value of three tests. At 25 and 7°C, greases A and B recorded a higher ECR, which gradually increased after ~30,000 strokes to levels of 30-60 percent and 15 percent, respectively. Greases C and D recorded much lower ECR (<2%) at both temperatures. At the lower temperatures minus-20 and minus-40°C),

greases A and B recorded very low ECR values (<5%). The ECR traces for greases C and D were very high and unstable.

The ECR measurement indicates a non-conductive material is formed in the interface. The ball-disc contact resistance varies with contact geometry, rubbing materials, tribofilm, and resistance of lubricant and wear particles. Therefore, if the ECR is low, it represents there is predominantly direct surface contact. However, if the ECR is high, it may indicate there is a high electrical resistance tribofilm [19] or wear particles formed in the contact [20]. These two cases will lead to either low or high wear respectively, because a tribofilm normally protects rubbing surfaces, but debris particles could accelerate abrasive wear. Further wear scar chemical analysis will help to identify whether it is a tribofilm or wear debris.

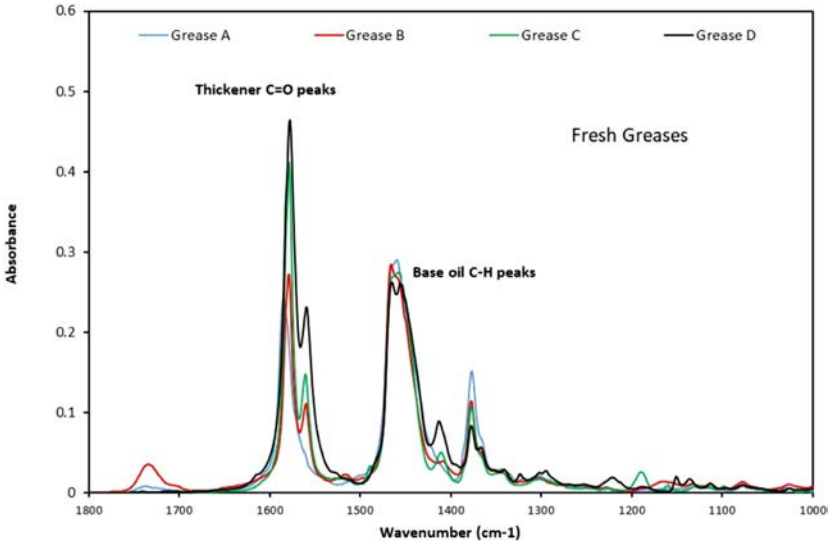

Figure 8: FTIR spectra of fresh greases.

The ball wear scar measurements are summarized in Figure 6. All the greases gave similar results at 25 and 7°C; however, at minus-20°C, grease D wear scar was significantly larger. At minus-40°C, greases C and D gave increased wear levels compared to A and B. The high wear recorded for greases C and D at the lowest temperatures corresponds to the high ECR levels recorded. This would suggest the ECR response is due to the formation of non-conductive wear debris [20] rather than additive film formation.

3.2 Microscope Images of Wear Scars

At the end of the test, the disc was not cleaned but retained with the grease film for further analysis. Initial inspection was by a low-powered microscope and examples are shown in Figure 7 for samples A and D tested at 25 and minus-40°C.

For most tests, grease is retained close to the wear scar where a thinner film is seen within the reciprocating zone. Outside this zone, the grease is undisturbed. The image for grease D at minus-40°C was strikingly different. The wear scar is seen clearly as the grease film appears to have retracted from the sheared region. Again, outside this zone, the grease is undisturbed.

Larger-scale magnification images of the A and D wear scars are shown later in the article with the Raman analysis (Figure 10). For grease D, the characteristic red-brown wear debris indicating haematite (Fe2O3) is clearly visible around the wear scar. This is indicative of fretting corrosion damage [5], [10], [12] and is probably the origin of the high ECR value measured for this test [20].

3.3 FTIR Results

The fresh grease spectra are shown in Figure 8 for a limited wavelength range of 1,800-1,000 cm^{-1}, as this region contains the most important peaks used to identify thickener, base oil, and additive grease components [16]. The spectra are plotted in Absorbance units, after normalization of the C-H peaks at ~1,460 cm^{-1}, as this allows for comparison of the thickener content.

The spectra of fresh greases were saved as reference for comparison with RA-IRS spectra of lubricant films in the wear scar. The strongest absorbance peaks are associated with the thickener and base oil components, while those due to additives are usually weak. Peaks at 1,580 and 1,560 cm^{-1} correspond to the asymmetric stretch vibrations of the carboxyl group (COO) in the hydroxystearate thickener [21]. The bands at ~1,464 and 1,377 cm^{-1} are various CH vibrations due to both base oil and thickener. From this relative comparison, the thickener content is approximately D>C>B>A. Any change to the composition of the grease film can be seen as a relative change in the component peak absorbance or loss compared to the spectrum of fresh grease [16], [21].

Post-test lubricant deposits in and around the disc wear track were examined by RA-IRS, and the results were compared to the reference fresh grease spectra. Figure 9 (upper) shows images from grease films after tests at minus-40°C; typical RA-IRS sample positions are indicated by red circles. The corresponding RA-IRS spectra are shown in Figure 9 (lower).

For all greases at higher temperatures (25 and 7°C), both thickener and base oil were present in the wear scar. The characteristic bands corresponding to thickener at 1,580 and 1,560 cm^{-1} can be seen in Figure 9 (upper) at 25°C for both A and D. Similar results were recorded for the 7°C tests. However, at lower temperatures, complete loss of the thickener peaks was seen for grease D at minus-20°C. Thickener was still present in the wear scar films for greases A, B, and C. At minus-40°C, thickener was present for grease A but not for greases C and D (Figure 9 lower). The RA-IRS results

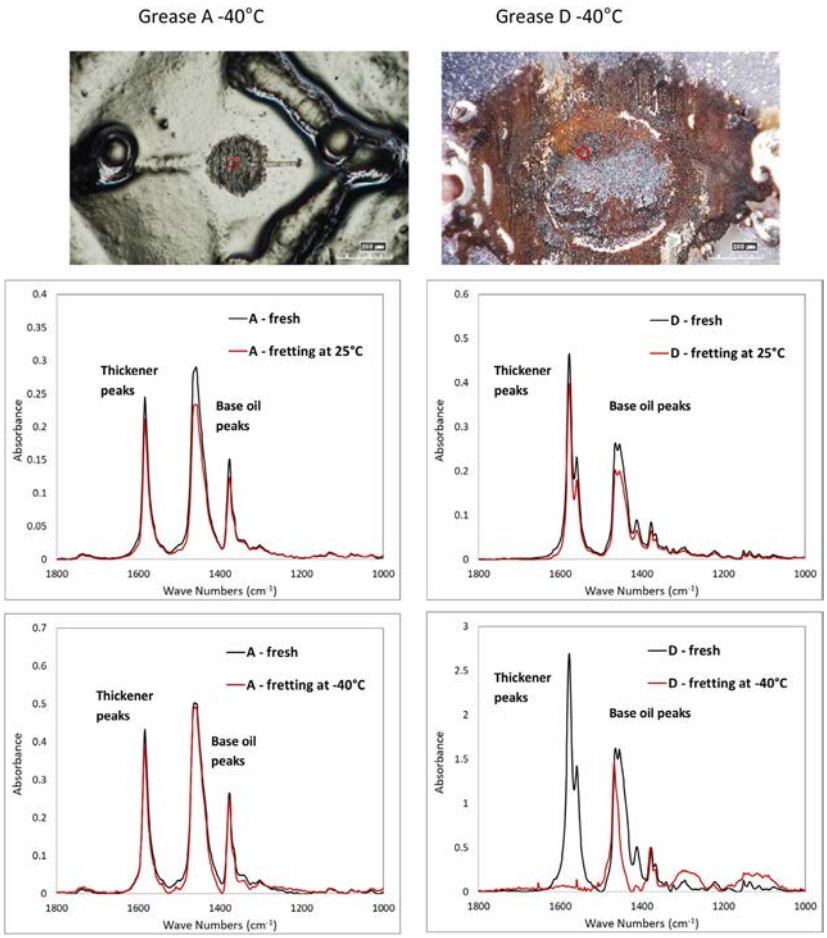

Figure 9: Upper: Microscope images for grease samples for A and D at minus-40°C indicating the area of RA-IRS analysis. Scale marker 250 µm: Lower: FTIR spectra of fresh and wear scar grease samples for A and D at 25 and minus-40°C. Grease A at minus-40°C. Grease D at minus-40°C.

for grease B at minus-40°C were ambiguous, although the grease gave relatively low wear (average WSD 250 µm), thickener was not identified in the wear scar. However, the spectra were poor quality, and clear interpretation is not possible due to baseline drift. Interestingly, although the thickener is absent for some greases at low temperatures base oil peaks (1,500-1,300 cm^{-1}) are still present, suggesting released oil reflow into the track is still occurring. The implications of these findings will be discussed in Section 3.5.

3.4 Raman Spectroscopy and SEM-EDS Analysis of Wear Scar Chemistry

Raman spectroscopy and SEM-EDS were used to investigate the surface chemistry of the disc wear tracks. After each HFRR test following the RA-IRS analysis, the discs were rinsed with toluene and air-dried. Any grease remaining in the wear tracks was washed away, so the Raman and EDS analysis was focused on the adherent tribofilm and wear debris. EDS analysis was carried out for different regions and representative results are shown. The results are presented as element composition in atomic percentage. Figure 10 and Figure 11 show example Raman spectra and SEM-EDS analysis for greases A and D at 25 and minus-40°C.

The SEM images provide evidence of different wear mechanisms. For grease A at 25°C (Figure 10 upper), the surface is grooved, which is characteristic of a predominately abrasive wear mechanism. The friction coefficient is low throughout the test (µ~0.15), while the ECR trace increases to 20-40 percent as the test proceeds. EDS results show some phosphorus and sulphur (0.01 at%), which might indicate formation of a non-conducting P/S additive film [19]. There were also high percentages of iron and oxygen confirming the iron oxides detected by Raman. It is worth noting the working depth of EDS is up to 5 µm depending on the accelerating voltage, but Raman scanning depth is from nanometers to 1 µm; while the thickness of anti-wear tribofilms are in nanometers. Therefore, it is reasonable that the percentage of iron was high, but sulphur and phosphorus content were low; in addition, chromium and carbon (resulted from oxidation/degradation of lubricants) were detected. In contrast, point 2 did not register sulphur and phosphorus. Instead, the relatively higher oxygen content clearly coincided with Raman results, suggesting the formation and accumulation of iron-oxide debris. The low wear (178.9 µm average ball WSD) is possibly due to the combination of additive film formation and the presence of thickener in the lubricant film as indicated by the RA-IRS results (Figure 9 lower).

In contrast, the wear scar for grease D at 25°C (Figure 10 lower) appears "plucked" with smeared regions, indicating adhesive wear and plastic deformation. The EDS analysis indicates high sulphur content (0.04 at%) in the wear scar, which is supported by peaks in the Raman spectra at 342/374 cm^{-1} tentatively assigned to an FeS film [22]. This analysis is further supported by the friction and ECR results. The friction coefficient is initially high and erratic (µ=0.5–0.7), dropping to a low stable value ~µ=0.18 after 20,000 strokes. The ECR value was low throughout most of the test. These observations, coupled with the relatively low wear value (247.2 µm average ball WSD), indicate the formation of an electrically conductive sulphur-containing additive film [22] as the test progressed.

The results for greases A and D at minus-40°C are shown

in Figure 11. Wear remained low for greases A and B (~250 µm) but increased significantly for greases C and D (400 and 500 µm respectively). Friction also increased for all greases, for A, C, and D, average friction coefficient was 0.5-0.8. Grease B was lower (~µ=0.3), but there was a large variation in results from the individual tests (µ=0.2-0.9).

For grease A, there appear to be compacted deposits in the wear track (Point 1 Figure 11 upper image). The EDS analysis indicates high carbon and fairly low oxygen content. The Raman spectra identify Fe_3O_4 (peak at 666 cm^{-1}) and possibly $\gamma - Fe_2O_3$ (1312 cm^{-1}). There is also an indication of organic content, possibly due to Ca thickener (CH ~ 2,427 and C O _ 1,570 cm^{-1}). This material has survived solvent cleaning and is tightly bound, possibly part of a transformed layer of wear debris and Ca thickener. The RA-IRS spectra also indicated the continued presence of thickener in the lubricant film. As such, it contributes to the low wear but relatively high friction measured for grease A. S/P films were not detected in the wear track.

The SEM image from grease D also shows deposits in the wear scar, although this appears to be more particulate. Low magnification images of the wear scar show red iron oxide deposits (Figure 9 lower), and this is supported by the Raman and EDS analysis. Fe_2O_3 (doublet 220, 281 cm^{-1}) was detected by Raman spectroscopy. In addition, high levels of oxygen (45-50 at%) were measured by EDS. The test also recorded very high and unstable ECR trace, which is due to non-conductive iron oxides formed during fretting wear [20] (Table 3).

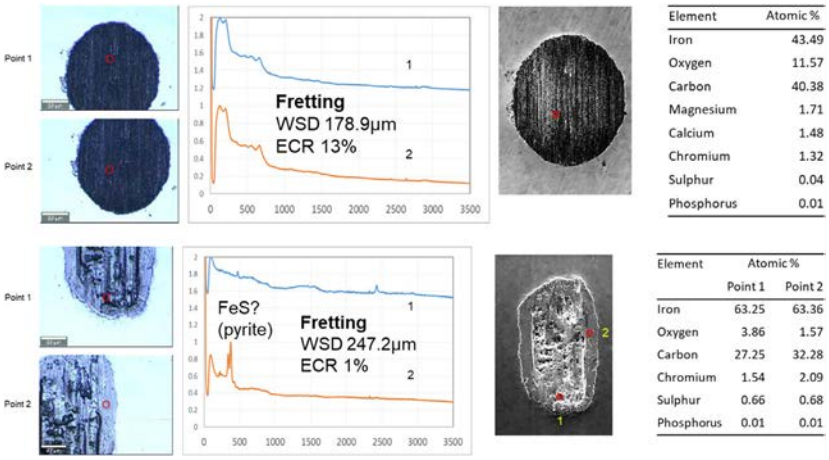

Element	Atomic %
Iron	43.49
Oxygen	11.57
Carbon	40.38
Magnesium	1.71
Calcium	1.48
Chromium	1.32
Sulphur	0.04
Phosphorus	0.01

Element	Atomic %	
	Point 1	Point 2
Iron	63.25	63.36
Oxygen	3.86	1.57
Carbon	27.25	32.28
Chromium	1.54	2.09
Sulphur	0.66	0.68
Phosphorus	0.01	0.01

Figure 10: Raman and SEM-EDS analysis on disc wear tracks from tests on from 25°C tests: upper grease A and lower grease D. Red circle shows analysis position. Scale marker: 60 µm.

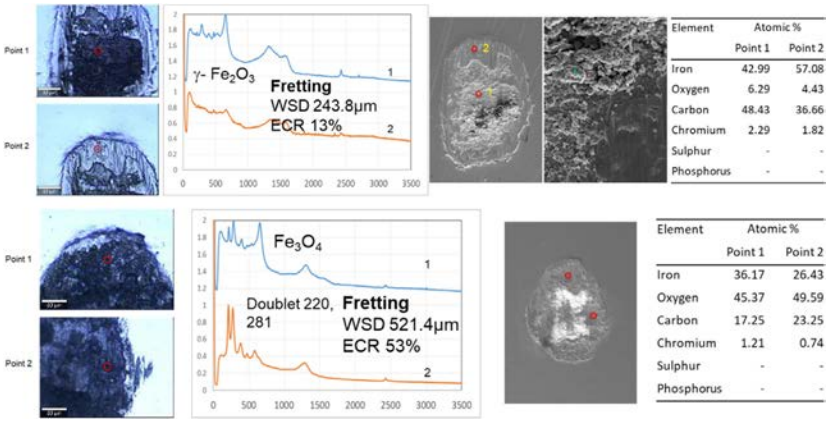

Element	Atomic %	
	Point 1	Point 2
Iron	42.99	57.08
Oxygen	6.29	4.43
Carbon	48.43	36.66
Chromium	2.29	1.82
Sulphur	-	-
Phosphorus	-	-

Element	Atomic %	
	Point 1	Point 2
Iron	36.17	26.43
Oxygen	45.37	49.59
Carbon	17.25	23.25
Chromium	1.21	0.74
Sulphur	-	-
Phosphorus	-	-

Figure 11: Raman and SEM-EDS analysis on disc wear tracks from tests on from –40°C tests: upper grease A and lower grease D. Red circle shows analysis position. Scale marker: 60 µm.

3.5 Discussion: lubrication mechanisms and implications for blade bearing grease formulation

The article reports friction and wear results for a range of commercial greases. Although the results are limited, it is possible to infer some relationship to grease composition. The greases had various calcium or lithium hydroxystearate/complex thickener systems at different concentrations. Some information on the thickener concentration can be gleaned from FTIR spectra of the fresh greases (Figure 8). The peak absorbance for the thickener (C_O ~1,580 cm^{-1}) relative to the base oil (C-H ~1,460 cm^{-1}) can be used to give a rough guide to thickener content.

The spectra were normalized to the CH peak absorbance so a direct comparison is possible and this indicates the thickener concentrations were ranked D>C>B>A. Similarly, for the base oil, there is limited information for the composition. The specified base oil viscosities varied from D (1,116 mm^2/s)>C (316 mm^2/s)>B (224 mm^2/s)>A (23.3 mm^2/s) at 25°C. It was possible to extrapolate base oil viscosities from

Summary of Raman peak results.

Grease	Peak position cm^{-1}	Assignment[18,22]
A 25 °C	210	Fe_2O_3
	666	Fe_3O_4
	342	FeS
D 25 °C	374	FeS
	666	Fe_3O_4
	2427	CH
A – 40 °C	666	Fe_3O_4
	1320	Fe_2O_3
	1571	C=O Ca thickener
	2427	CH
D – 40 °C	220	Fe_2O_3
	280	Fe_2O_3
	666	Fe_3O_4
	1300	Fe_2O_3
	2427	CH

Table 3: Summary of Raman peak results.

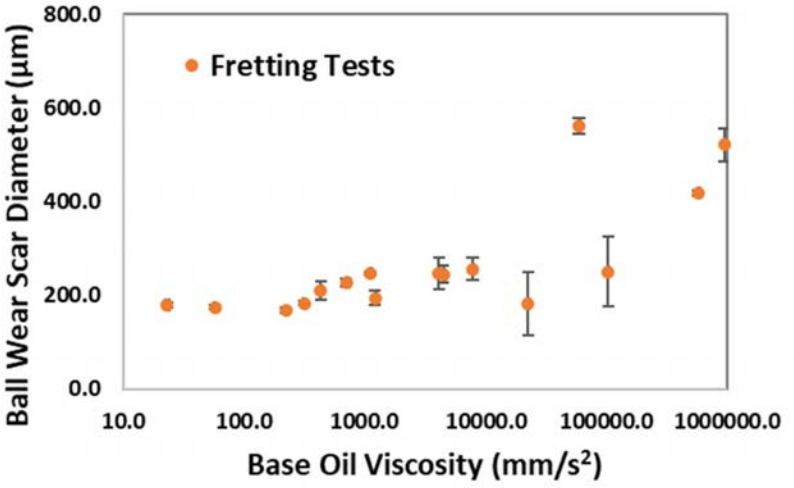

Figure 12: Wear scar diameter plotted against base oil viscosity for all greases and temperatures.

published data for all the test temperatures using ASTM plots and this is summarized in Table 2. The FTIR analysis suggests that greases A and B have a synthetic base oil with an ester component (peak at 1,735 cm^{-1}). It is assumed all greases contained a range of additives and evidence of P- and S-containing reacted films was obtained in the EDS analysis.

Differences were recorded in the measured wear at the lower temperatures, and this can be related to the grease composition and mechanism of film formation. Wear performance was better for the lower viscosity base oil and lower thickener-content greases. The relationship of measured wear generally increases with base oil viscosity as shown in Figure 12, which is the inverse of the usual EHL film thickness "rules."

Further evidence for the lubrication mechanism comes from the RA-IRS analysis of the film remaining in the wear scar at the end of the tests. At higher temperatures (25, 7°C), thickener was present in lubricant film for all greases, and correspondingly similar low friction and wear results were recorded. At the lower temperatures, thickener peaks were absent for greases C (minus-40°C) and D (minus-20, minus-40°C), although a thin film of free oil was present, and this condition was associated with much higher wear. The anomaly in this analysis was grease B, which had low wear at minus-40°C but with no apparent thickener present. However, the analysis also showed the presence of an ester component in the lubricant film, which might contribute to enhanced friction and wear properties in the absence of the thickener [23].

In the classical grease lubrication model, it is usually assumed that "bled" oil released by shear-degradation of bulk grease replenishes the track and forms the lubricating film [24] [25]. However, this model was developed for bearings operating at fairly high speeds and either unidirectional or long amplitude reciprocation. An alternative model suggested by Scarlett [26] was that grease deposits a high-viscosity thickener layer in the track. Evidence of both mechanisms has been demonstrated in the laboratory in ball-on-disc tests [25], [27]. For slow-speed fretting contacts, the entrainment and retention of thickener is likely to be a factor. Under these conditions, the formation of a hydrodynamic film is inhibited both due to the low speed (hc~ entrainment speed0.7) and the fretting condition. The fretting condition means provision of fluid is restricted as, at stroke reversal, the contact moves back into the depleted exit region. Lubricant replenishment close to the contact, in the absence of excess fluid, is driven primarily by capillary and surface-tension forces [28][29]. Although released oil was present as a thin (estimate ~µm) film in the scars for high-wear tests, this suggests the base oil alone does not provide sufficient surface protection under these conditions. It is also probable that S/P additives do not work at very low temperatures, as these elements were not detected in the minus-40°C EDS film analysis (Figure 11) but were present at higher temperatures (Figure 10). Reflow-driven replenishment is reduced for high-base oil viscosities and grease [29] [30], and this will be exacerbated at low-temperatures. The EDS analysis also showed higher carbon levels for grease A compared to grease D at low temperatures, which correlates with low wear and supports the conclusion that the thickener contributes to load-carrying.

There is an apparent contradiction in this statement as low wear correlated with the lower thickener-content greases. In ball-on-disc unidirectional tests, entrainment of bulk grease into the contact produces much thicker lubricant films than predicted from the base oil viscosity, particularly at low speeds, and has been demonstrated for a range of thickener types [26], [27], [31]. Thus, the thickener will contribute to enhanced load-carrying for low-temperature fretting where the hydrodynamic film is restricted and additive action inhibited.

To explain the low wear/low thickener content contradiction, it is worth considering grease lubrication mechanisms in the fretting regime. At the start of the HFRR test, the ball is loaded onto a 50 µm thick grease film; some grease will be trapped in the contact, but most will be pushed up around the ball. As reciprocation starts, grease in the contact is rapidly broken down; this is often seen as an increase and then rapid decrease in ECR. Bulk grease closest to the ball will be displaced by the reciprocating action and shear-degraded releasing mobile fluid [25] facilitating contact replenishment. The presence of released base-oil in the track has been shown for some of the low-temperature tests. We suggest this is an underlying mechanism, which occurs for all conditions, but it is augmented by bulk-grease replenishment in

the low-wear tests. For small-amplitude motion, it is feasible that displaced grease adhering to the ball is pulled back into the track during reciprocation. Thus, there is a mechanism to continually supply grease to the track, and this might be related to the bulk properties which include rheology (yield stress, visco-elasticity), adherence and tackiness. The apparent contradiction in the low wear/low thickener conclusion can thus be explained by considering the properties that determine grease retention around the contact rather than the absolute thickener-concentration. It is the ability of the grease to maintain replenishment of the contact that is important, and lower base oil viscosity and thickener content would aid this. Thus, yield stress, visco-elasticity, and adherence/tackiness properties could all play a role. "Tackiness" is the property used to describe the ability of a grease to form "strings" when a small sample is retracted [32], and this might contribute to replenishment. The "adherence" model of replenishment is supported by the image in Figure 7 (lower images) where grease D at minus-40°C has clearly retracted from around the wear scar. Very high wear (ball scar diameter > 500 µm) and friction (average µ~0.8) were recorded in this test. Grease A at minus-40°C is still retained close to the contact and recorded much lower wear (ball scar diameter ~250 µm) and friction (average µ~0.6). The RA-IRS spectra also showed thickener to be present in the lubricant film. As such, it contributes to the low wear but relatively high friction measured for grease A.

A key question is whether these results and proposed lubrication mechanism are applicable to blade pitch bearing operation. The HFRR test conditions of low frequency, restricted stroke amplitude, and high pressure replicate those found in practice. In bearings, there are additional mechanical forces that contribute to replenishment of the track; these include cage effects [33], lateral vibration [34], and transient loading [35][36]. All of these can aid bulk grease movement; however, in the confined fretting motion, it is possible that the adherence mechanism also operates.

The results presented in this article emphasize the complexity of grease lubrication of fretting contacts at low temperatures. Grease lubrication performance is strongly linked to contact replenishment, which depends critically on the test configuration and operation. In fretting tests, we suggest lubricant replenishment is a mixture of released-oil reflow and bulk grease adherence. The efficiency of the reflow mechanism will be determined by the amount of fluid released during shear and the viscosity/polarity of the fluid. Increasing base oil viscosity might increase fully-flooded EHL film thickness, and hence reduce wear, but if it hinders lubricant replenishment of the contact, the inverse occurs. In the current work, increasing base oil viscosity was linked to higher wear and incorporating a low viscosity; polar component in the base oil might facilitate replenishment or low friction behavior.

4 CONCLUSIONS

Fretting tests have been carried out to measure the friction and wear performance of four commercial wind turbine greases, for a range of temperatures (25, 7, minus-20, minus-40°C). Similar friction and wear performance was recorded for all the greases at the higher temperatures (25 and 7°C). At the lowest temperature, greases C and D gave markedly poorer results. Overall, for the temperature range tested, the best friction and wear results were for the grease formulated with the lowest viscosity base oil. In low-temperature, fretting contacts base oil replenishment does not provide sufficient surface protection. The presence of thickener in the track also appears to contribute to wear reduction, which suggests bulk grease must be periodically supplied to, or retained in, the track. The "adherence" replenishment mechanism will be linked to the grease rheology and/or tackiness, which will be critically temperature dependent. The contribution of S/P anti-wear additives at low temperatures is unclear and requires further investigation.

STATEMENT OF ORIGINALITY

The research work described in this paper is, to the best of the authors' knowledge and belief, original, except as referenced and acknowledged in the text. The work has not been submitted elsewhere, either in whole or in part, for publication.

DECLARATION OF COMPETING INTEREST

The authors declare that they have no known competing financial interests or personal relationships that could have appeared to influence the work reported in this paper.

DATA AVAILABILITY

Data will be made available on request.

ABOUT THE AUTHORS

Jie Zhang and Philippa Cann are with the Tribology Group, Imperial College London. Alan Wheatley and Sarah Matthews are with Shell Global Solutions (UK) Shell Research Ltd. Rihard Pasaribu is with Shell Downstream Services International B.V, Netherlands. Edward Worthington and Caroline Zinser are with Shell Global Solutions (Deutschland) GmbH, Hamburg, Germany.

REFERENCES

[1] https://wwindea.org/world-market-for-wind-power-saw-another-record-year-in-2021-973-gigawatt-of-new-capacity-added; accessed 26 September 2022.

[2] A. Dhanola, H.C. Garg; Tribological challenges and advancements in wind turbine bearings: a review. Eng Fail Anal, 118 (2020), Article 104885.

[3] M. Stammler, P. Thomas, A. Reuter, F. Schwack, G. Poll; Effect of load

reduction mechanisms on loads and blade bearing movements of wind turbines; Wind Energy, 23 (2020), pp. 274-290.

[4] M. Stammler, A. Reuter, G. Poll; Cycle counting of roller bearing oscillations – case study of wind turbine individual pitching system; Renew Energy Focus, 25 (2018), pp. 40-47.

[5] A.M. Kirk, P.H. Shipway, W. Sun, C.J. Bennett; Debris development in fretting contacts – debris particles and debris beds; Tribology Int, 149 (2020), Article 105592.

[6] P.M. Cann; Thin-film grease lubrication; Proc Inst Mech Eng, Part J: J Eng Tribology, 213 (5) (1999), pp. 405-416.

[7] ASTM D4170: Standard Test Method for Fretting Wear Protection by Lubricating Greases.

[8] ASTM D7594 - Fretting Wear Resistance of Lubricating Greases Under High Hertzian Contact Pressures Using a High-Frequency, Linear-Oscillation (SRV) Test Machine.

[9] https://issuu.com/kim0824/docs/6_nov_dec_2020/52 (accessed 11 October 2022).

[10] F. Schwack, N. Bader, J. Leckner, C. Demaille, G. Pol; A study of grease lubricants under wind turbine pitch bearing conditions; Wear, 454–455 (2020), Article 203335.

[11] T. Maruyama, T. Saitou, A. Yokouchi; Differences in mechanisms for fretting wear reduction between oil and grease lubrication; Tribol Trans, 60 (2016), pp. 497-505.

[12] Z.R. Zhou, L. Vincent; Lubrication in fretting — a review; Wear, 225–229 (1999), pp. 962-967.

[13] ASTM D6079-11; Test method for evaluating lubricity of diesel fuels by the high-frequency reciprocating; Rig (HFRR) (2016).

[14] ISO 12156-1; Diesel fuel – assessment of lubricity using the high-frequency reciprocating; Rig (HFRR) (2016).

[15] K.L. Johnson; Contact Mechanics; Cambridge University Press (1985).

[16] P.M. Cann, M.N. Webster, J.P. Doner, V. Wikstrom, P. Lugt; Grease degradation in ROF bearing tests; Tribology Trans, 50 (2007), pp. 187-197.

[17] P.M.E. Cann, A.A. Lubrecht; Bearing performance limits with grease lubrication: the interaction of bearing design, operating conditions and grease properties; J Phys D: Appl Phys, 40 (18) (2007), pp. 5446-5451.

[18] D.L.A. de Faria, S. Venancio Silva, M.T. de Oliveira; Raman microspectroscopy of some iron oxides and oxyhydroxides; J Raman Spectrosc, 28 (11) (1997), pp. 873-878.

[19] J.L.Hernández Viesca, A. Battez, A.R. González, T. Reddyhoff, A. Torres Pérez, H.A. Spikes; Assessing boundary film formation of lubricant additivised with 1-hexyl-3-methylimidazolium tetrafluoroborate using ECR as qualitative indicator; Wear, 269 (2010), pp. 112-117.

[20] M. Varenberg, G. Halperin, I. Etsion; Different aspects of the role of wear debris in fretting wear; Wear, 252 (2002), pp. 902-910.

[21] Hurley, S. and Cann, P.M. IR Spectroscopic Analysis of Grease Lubricant Films in Rolling Contacts, 25th Leeds-Lyon Symposium on Tribology (1999): 589-600.

[22] B. Li, L. Huang, M. Zhong, Z. Wei, J. Li; Electrical and magnetic properties of FeS2 and CuFeS2 nanoplates; RSC Adv, 5 (2015), pp. 91103-91107.

[23] G. Guangteng, H.A. Spikes; Fractionation of liquid lubricants at solid surfaces; Wear, 200 (1–2) (1996), pp. 336-345.

[24] E.R. Booser, D.F. Wilcock; Minimum oil requirements of ball bearings; Lubr Eng, 9 (140–3) (1953), pp. 156-158.

[25] Merieux, J.-S., Hurley, S., Lubrecht, A.A. and Cann, P.M. Shear Degradation of Grease and Base Oil Availability in Starved EHL Lubrication, Proc. 26th Leeds-Lyon Symposium on Tribology, Tribology Series (2000) 38: 581–588.

[26] Scarlett, N.A., Use of grease in rolling bearings Proc. IMechE., (1967) 182 (3A):167–171.

[27] P.M. Cann; Starved grease lubrication of rolling contacts; Tribology Trans, 42 (4) (1999), pp. 867-873.

[28] L. Huang, D. Guo, S.Z. Wen; Starvation and reflow of point contact lubricated with greases of different chemical formulation; Tribology Lett, 55 (2014), pp. 483-492.

[29] B. Jacod, F. Pubilier, P.M.E. Cann, A.A. Lubrecht; An analysis of track replenishment mechanisms in the starved regime; Tribol Ser, 36 (1999), pp. 483-492.

[30] L. Gershuni, G. Mats, M.G. Larson, P.M. Lugt; Lubricant replenishment in rolling bearing contacts; Tribol Trans, 51 (2008), pp. 643-651.

[31] M. Gao, H. Liang, W. Wang, H. Chen; Oil redistribution and replenishment on stationary bearing inner raceway; Tribol Int, 165 (2022), Article 107315.

[32] S. Achanta, M. Jungk, D. Drees; Characterisation of cohesion, adhesion, and tackiness of lubricating greases using approach–retraction experiments; Tribol Int, 44 (2011), pp. 1127-1133.

[33] B. Damiens, A.A. Lubrecht, P.M. Cann; Influence of cage clearance on bearing lubrication; Tribology Trans, 47 (1) (2004), pp. 2-6.

[34] Y. Nagata, K. Kalogiannis, R. Glovnea; Track replenishment by lateral vibrations in grease-lubricated EHD contacts; Tribol Trans, 55 (2012), pp. 91-98.

[35] P.M. Cann, A.A. Lubrecht; The effect of transient loading on contact replenishment with lubricating greases; Tribology Ser, 43 (2004), pp. 745-750.

[36] X. Zhang, R. Glovnea; An experimental investigation of grease lubricated EHD contact subjected to normal sinusoidally variable loading; Tribol Int, 147 (2020), Article 106272.